Chemistry and Materials Research
ISSN 2224- 3224 (Print) ISSN 2225- 0956 (Online)
Vol.8 No.6, 2016

Synthesis and Characterisation of Copper Oxide Thin Films Using Successive Ionic Layer Adsorption Reaction (SILAR) Method

R. Daniel-Umeri[1] R.U. Osuji[2] F.I Ezema[2]
1. Department of Science Laboratory Technology, Delta State Polytechnic, Ozoro, Delta State, Nigeria
2. Department of Physics and Astronomy, University of Nigeria, Nsukka

Abstract
Cu_xO thin films were synthesized on glass substrate by using a simple chemical method; successive ionic layer adsorption reaction (SILAR). The effects of bath pH and temperature on the structural, morphological and optical properties of the films were investigated. The films were prepared by successively dipping them for 20 s each in a solution of 1 M NaOH and then in a solution of 0.1M copper complex. Temperature of the NaOH solution was varied from room temperature to 70^{o}C, while that of the copper complex solution was maintained at room temperature. The films were characterized by X-ray diffraction (XRD), scanning electron microscopy (SEM) , ultraviolet-visible spectroscopy (UV-VIS) and fourier transform infrared (FTIR) spectroscopy. XRD studies confirmed that the films were polycrystalline with both Cu_2O and CuO crystallographic phases existing depending on the pH of the solution bath. The calculated crystallite size from the XRD measurement was found to be in the range ~1.52 - 1.67Å. SEM micrograph revealed that the grains were distributed evenly over the substrate surface. The bandgap value was found to be in the range, 1.6eV-2.0 eV.
Keywords: Copper Oxide, SILAR, pH, Temperature.

1. Introduction

Copper oxide, including cuprous oxide and cupric oxide is formed when copper is exposed to oxygen and oxidizes. These semiconductor oxides have been studied for several reasons such as: the natural abundance of starting material (Cu); the easiness of production by Cu oxidation; their non-toxic nature and the reasonably good electrical and optical properties exhibited by Cu_2O [1].

Reports from previous works showed that many of the growth methods for cuprous oxide resulted in a combined growth of copper (I) oxide Cu_2O and copper (II) oxide CuO [2].

Cupric oxide (CuO) has a monoclinic crystal structure with a band gap of 1.22–2.0 eV [3,4]. Cuprous oxide (Cu_2O) has a cubic crystal structure with a bandgap of 2.10 to 2.60 eV [5, 6] . Its high optical absorption coefficient in the visible range and reasonably good electrical properties constitute important advantages and render Cu_2O as the most interesting phase of copper oxides [7]. CuO and Cu_2O materials are known to be p-type semiconductors in general and hence potentially useful for constructing junction devices such as pn junction diodes [8]. Apart from their semiconductor applications, these materials have been employed as heterogeneous catalysts for several environmental processes [9], solid state gas sensor heterocontact [10] and microwave dielectric materials [11]. Their use in power sources has received special attention. Thus, in addition to photovoltaic devices [12], copper oxides have been used as electrode materials for lithium batteries [13]

The different physical and chemical techniques that have been utilized to grow copper oxide thin film on glass include , the anodic oxidation of copper through a simple electrolysis process [14] method [15], spray pyrolysis [16], r.f. magnetron sputtering [17], reactive evaporation [18], sol-gel method [19], [Electrodeposition [20, 21], chemical vapor deposition [23], plasma evaporation [24], and chemical deposition methods [25].

Cupric oxide (CuO), on the other hand, is a *p*-type semiconductor having a band gap of 1.21–2.0 eV and monoclinic crystal structure [19-23]. It has been widely used in various applications, such as dye-sensitized solar cells [24], heterogeneous catalyst [25], gas sensors [26] and lithium-copper oxide electrochemical cells [27].The potential of copper oxide films as spectrally selective variable reflectance coatings for radiant energy control in architectural and aerospace applications has been highlighted by Richardson et al. (2000) [16].
The physical properties of the obtained films seem to be very sensitive to the detailed arrangement of Cu and O atoms, which in turn is influenced by the deposition method and the particular conditions.
In this paper, our emphasis is mainly focused on the effect of pH and bath temperature on the optical, structural and surface morphological properties of Cu_xO thin films deposited by SILAR method.

2. Experimental Procedures

Prior to the deposition of Cu_xO thin film on microscope glass slide substrates, the substrates were cleaned thoroughly to avoid any surface contamination. The glass substrates were kept overnight in a mixture of chromic and sulphuric acid, it was then washed with detergent (soap solution), This was followed by cleaning the substrate in equivolume mixture of acetone and ethanol and finally rinsed with distilled water. It was then hung in air for it to dry.

For the preparation of Cu_xO thin film, the cationic precursor was 0.1M copper sulphate pentahydrate

($CuSO_4.5H_2O$) this was obtained by dissolving 1.25g in 50cm^3 distilled water while the anionic precursor was obtained by dissolving 2.0g of sodium hydroxide in 50cm^3 of distilled water to get 1M of the solution.

Solution of copper sulphate complex was prepared by adding Ammonia (NH_3) to copper sulphate solution until it turns deep blue.

To deposit nanocrystalline Cu_XO thin film, one SILAR cycle involves the following four steps: a well-cleaned glass substrate was first immersed into cationic precursor (vessel1) (0.1M copper complex solution at pH ~8 kept at room temperature) , so the Cu^{2}+ ions were adsorbed onto the substrate surface; (ii) then the substrate was rinsed with distilled water to remove loosely bonded Cu^{2}+ ions from the substrate; (iii) further, the substrate was immersed into anionic precursor (vessel 3) (1 M hot *NaOH* solution) maintained at 70^oC, this temperature was achieved by making use of a constant temperature bath, so OH^{2-} ions were adsorbed and reacted with Cu^{2}+ ions (iv) again the substrate was rinsed with distilled water to remove unadsorbed and unreacted OH^{2}– ions from the substrate. Thus, one SILAR cycle is completed. Therefore, we obtained a Cu_XO film by repeating such SILAR cycles 80 times. The anionic and cationic immersion times were 20 s and the rinsing time was 10s. After deposition, the films were rinsed with copious amounts of distilled water, dried with a hand drier and kept in an air tight container to avoid contamination. This procedure was also done for both anionic and cationic precursors kept at room temperature. The reaction occurring on the substrate surface can be represented as:

$2Cu+2OH-\rightarrow Cu_2O+H_2O$

The films were prepared for different pH (9, 10, 11, and 12) values of the copper sulphate complex.

The as-deposited thin films of Cu_XO were characterized for optical and surface morphological studies. The elemental composition was determined by EDAX technique. The surface morphology was studied by scanning electron microscopy (SEM, JOELJSM-5600). Absorbance spectra were recorded in the range 200–1100 nm by means of a JENWAY 6405 UV-VIS spectrophotometer.

The crystallographic orientation as well as structure of the deposited films were studied using X-ray diffractometer (Model Bruker D8 advance AXS) with scanning angles in the range 20–75° using CuK_α radiation (λ = 1.5406 Å).

The FTIR transmission spectra were recorded using a SHIMADZU 8400S spectrophotometer in the spectral range 500 - 4500 cm^{-1}.

3. Results and Discussion

3.1 Morphological Studies of the Deposited Films

Fig. 1(a-c) shows the SEM images of CuO nanostructures synthesized at room temperature from solutions with different pH values. The film shows uniform surface morphology without any pinholes and cracks. It can be observed that the pH value of the solution strongly affects the obtained morphology. The copper oxide structure prepared at pH 8 is obtained in the form of compacted crystalline grains with some overgrown clusters. This overgrowth can be explained on the basis of nucleation and coalescence process. As the pH increased to 9, the nanograins colour became brighter and more dispersed, and finally the deposit at pH 11 showed a network-like CuO nanofibres.

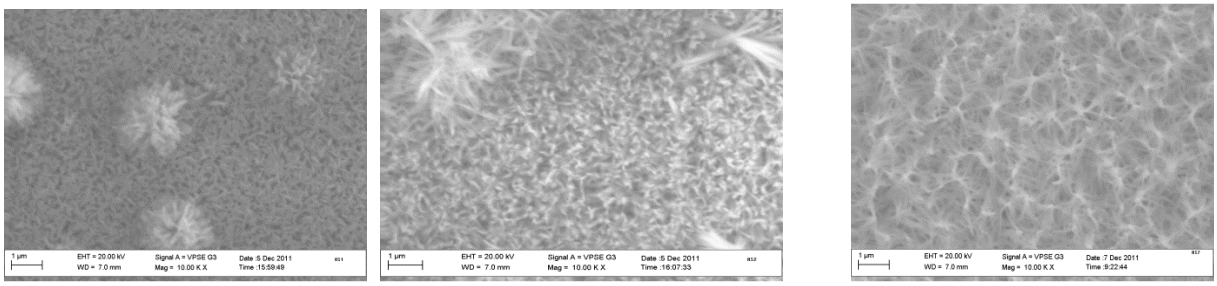

(a) (b) (c)

Fig.1 Scanning electron micrograph of Copper oxide thin film deposited at room temperature(a)pH 8 (b)pH 9(c) pH 11

Fig. 2 (a-b) illustrates the influence of heating the solution bath of the Anionic precursor to 70^{o}C on the obtained morphology. At pH 9 a fiber-like nanostructure that is an exact image of fig 5 (c) was observed and as the pH was increased to 11, well developed interconnected nanofibres is seen. There was also enhancement in the length of the fibers as well the packing density. The temperature dependence of the obtained morphology is likely due to the temperature dependence of the relative supersaturation [30]. For the same concentration, relative supersaturation is expected to decrease as the temperature increases.

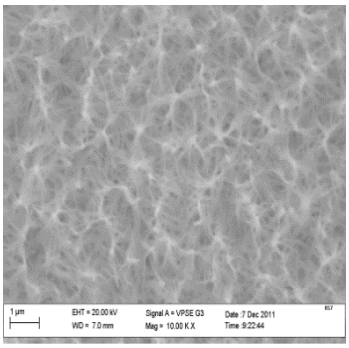

(a)

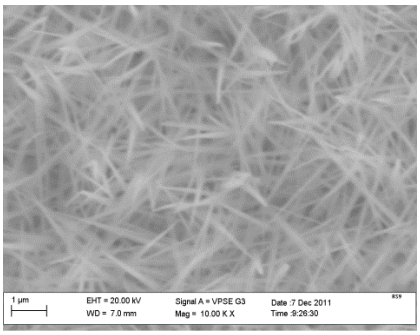

(b)

Fig 2. Scanning electron micrograph of Copper oxide thin film deposited at pH 9 and 11 with anionic precursor heated to 70^0 c

3.2 Compositional Analysis

Energy dispersive X-ray analysis (EDAX) spectroscopy measurement was used to determine the quantitative analysis and stoichiometry of the as- deposited film. Fig. 3 showed a typical EDAX spectrum of CuO deposited on glass substrate for both the films deposited at room temperature and at an anionic temperature bath of 70°C. It showed the presence of copper (Cu), oxygen (O) and the presence of other elements like Si and Ca, which are from the glass substrate.

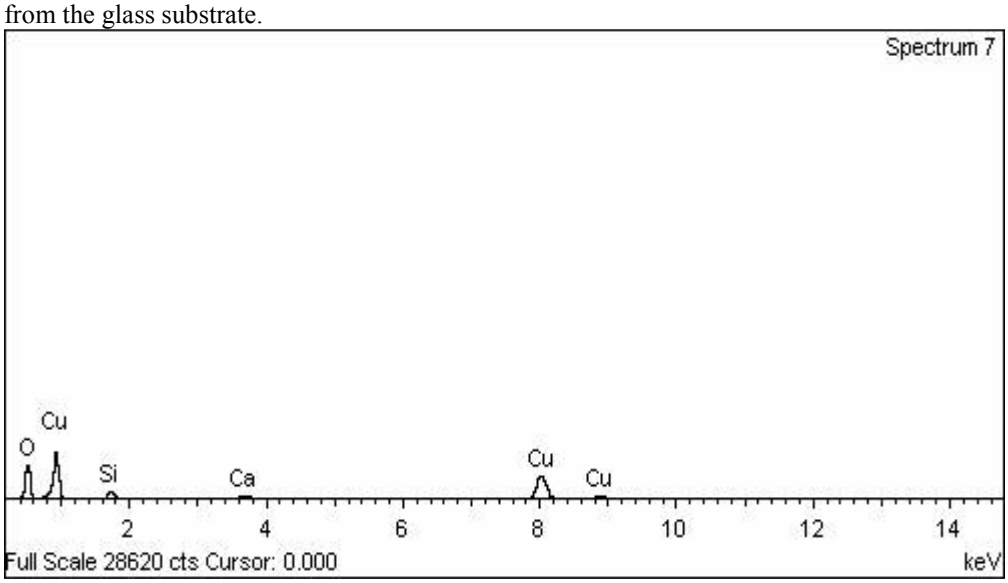

fig.3 EDX Spectrum for CuO

3.3 Optical Studies

3.31 UV-VIS Spectroscopy

Data obtained from optical characterization of the films were used to plot graphs for the absorbance, transmittance and optical band gap of the copper oxide thin film.

Fig. 4 (a) shows the optical absorption spectra of CuO film deposited at room temperature on glass substrate for pH 8, 9, 11. The figure shows that absorbance decays exponentially with an increase in wavelength. The spectra also revealed that the absorbance of the CuO films increases as the pH of the cationic precursor increases. It has been reported that the optical absorption would be affected considerably by the morphology and crystallinity of Cu_2O crystals [29].

Fig. 4 (b) shows the effect of heating the anionic bath temperature, on the absorbance of the copper oxide thin films. The curve showed a shift of the absorption edge to VIS and NIR regions. This shift indicates decrease in band gap, which can be attributed to increase in the thickness and in grain size with bath temperature. The spectral also reveals that the absorbance decreased with increase in the pH value.

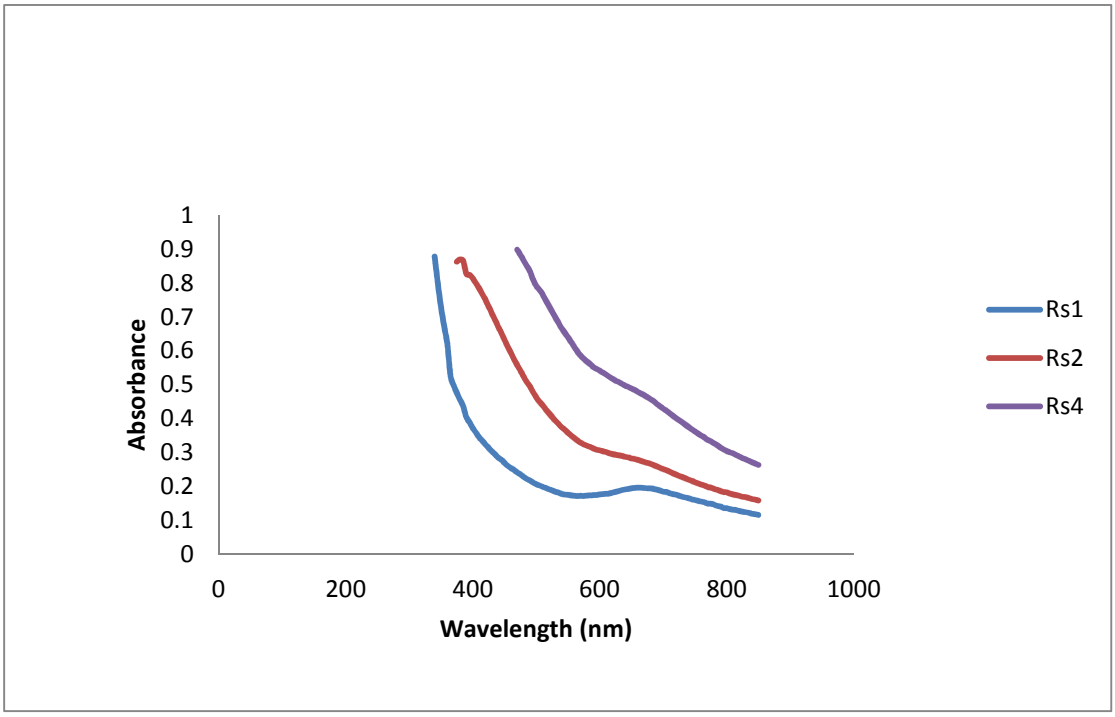

Fig 4 (a) Graph of Absorbance vs Wavelength for copper oxide deposited at room temperature.RS1= pH8, RS2= pH9, RS4= pH11

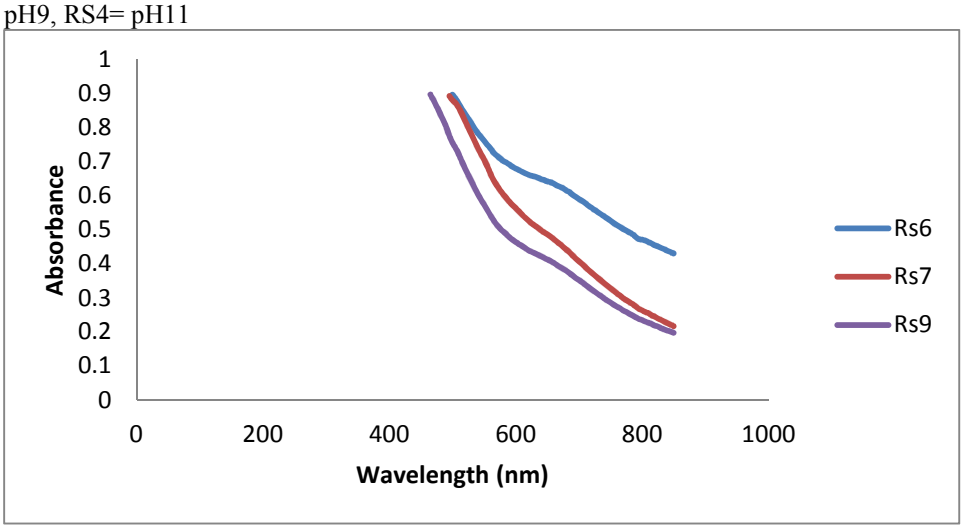

Fig 4.(b) Graph of Absorbance vs Wavelength for copper oxide deposited 70°C. RS6= pH 8, RS7= pH9 and RS9= pH11.

Transmittance spectra recorded for CuO films as a function of wavelength range 300 – 1000 nm indicate that the transmittance decreases with increase in the pH value for films deposited at room temperature for both precursors, while for films obtained by heating the anionic precursor to 70°c, shows that the transmittance of CuO films increase with increase in pH values of the copper complex solution.

Fig. 5(a) shows the plot of $(\alpha hv)^2$ vs. hv for films deposited at room temperature, while fig. 5(b) shows the plot of films deposited by heating the anionic precursor to 70°C. The value of the optical band gap has been determined from the value of the intercept of the straight line at a $(\alpha hv)^2 = 0$. The as-deposited CuO thin film optical band gap energy is calculated to be 2.0eV, 1.8eV and 1.6 eV for samples Rs2, Rs3 and Rs4 respectively. While for samples Rs6, Rs7 and Rs9, it is 1.85eV, 1.9eV and 2.0 eV respectively. These band gap values range of falls within the one reported by [16-21] for Cu_2O.

In this investigation, the band gap of films obtained at room temperature decreased as the pH increased while the band gap increased as the pH increased for films deposited at an anionic bath temperature of 70°c

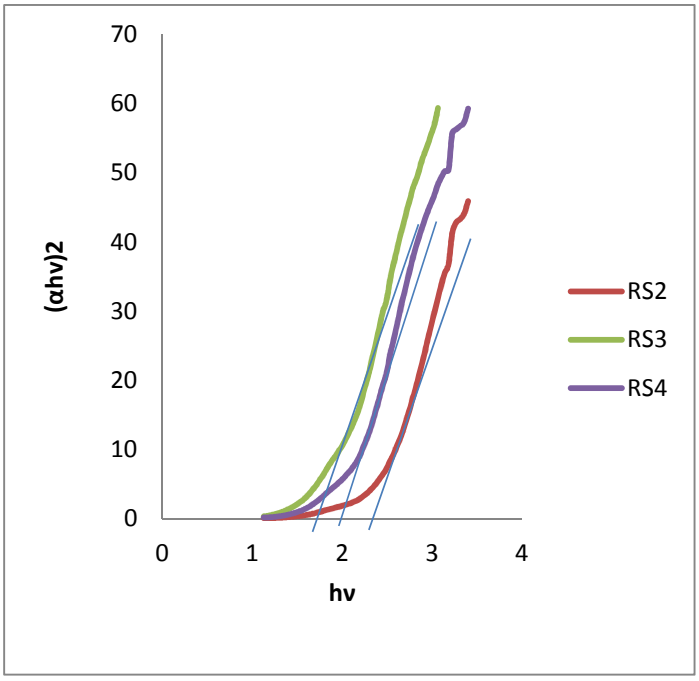

Fig. 5(a) Optical Band Gap of Cu_xO Deposited At Room Temperature . RS2=p H 8, RS3= p H 9, RS4 p H 11

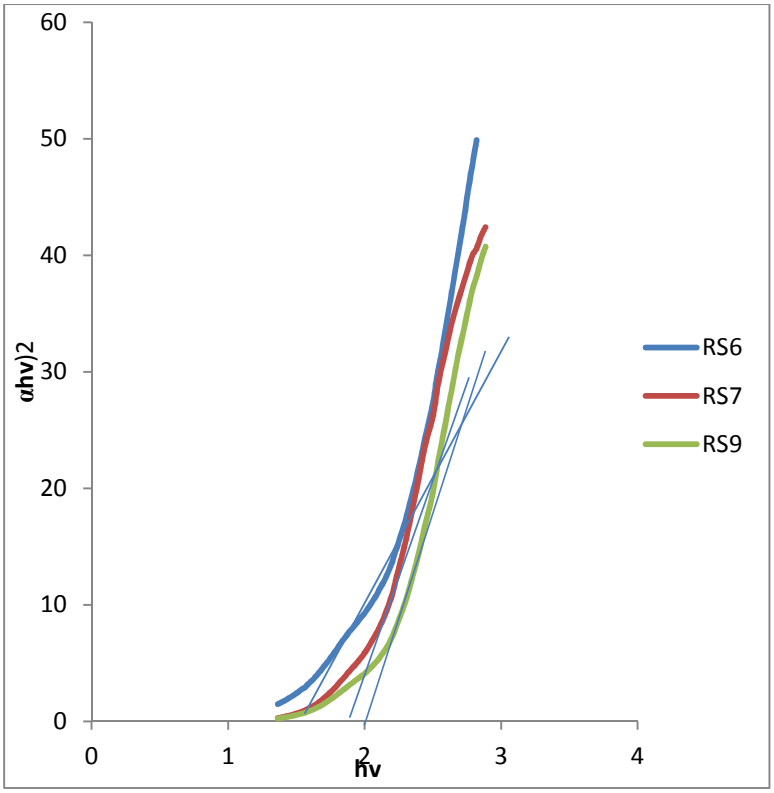

Fig. 5(b) Optical Band Gap ofCu_xO Deposited at a temperature of 70°c of the Anionic Precursor

A summary of the determined optical band gap values for copper oxides are shown in Table 1. The band gaps of films that were deposited at room temperature showed a decrease in bandgap as the pH value increased. In the case of the films deposited at an anionic bath temperature of 70°c, the band gap increased as the pH increased. This might be as a result of the change in the composition from Cu_2O to CuO.

Table1. Optical band gap (Eg) values for copper oxide thin films

Copper Oxide Thin Films Deposited at room Temperature	**Energy Band Gap (Eg)**
RS2=pH 9	2.0 eV
RS3=pH 10	1.8 eV
RS4=pH 11	1.6 eV
Copper Oxide Thin Films Deposited at a Temperature Bath of 70ºc	
RS6=pH 8	1.85eV
RS7=pH 9	1.9 eV
RS9=pH 11	2.0 eV

3.32 FTIR analysis

The Fourier transform infrared spectra of CuO were recorded in the region, 500-4500 cm^{-1}. Fig. 6 (a) shows the spectra of CuO deposited at room temperature, while fig. 6 (b) shows the spectra of the film deposited at an anionic bath temperature of 70ºC .In both spectra, the strong bands centered at 3569 cm^{-1}, 3303 cm^{-1} and 3571 cm^{-1} , 3303 cm^{-1} can be assigned to structural OH- groups and to water molecules in the interlamellar space, respectively .

The absorption peaks at 650 cm^{-1} (6a) and 623 cm^{-1} (6b) can be attributed to the Cu (I)-O vibration. Other peaks observed in the transmittance range from 1300 to 1800cm^{-1} can be attributed to the number of the vibrational modes

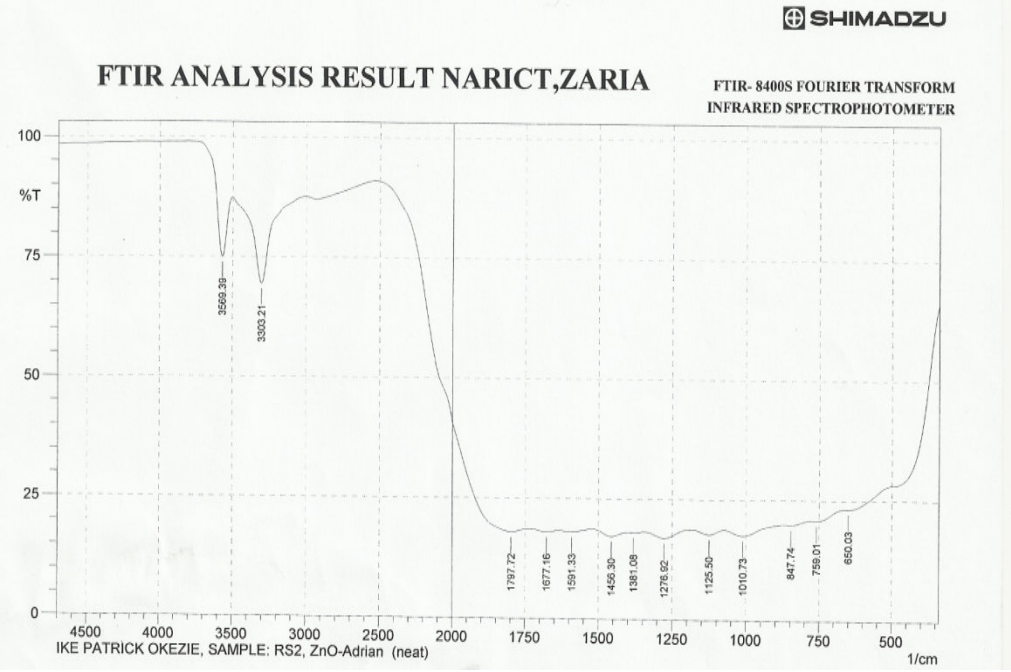

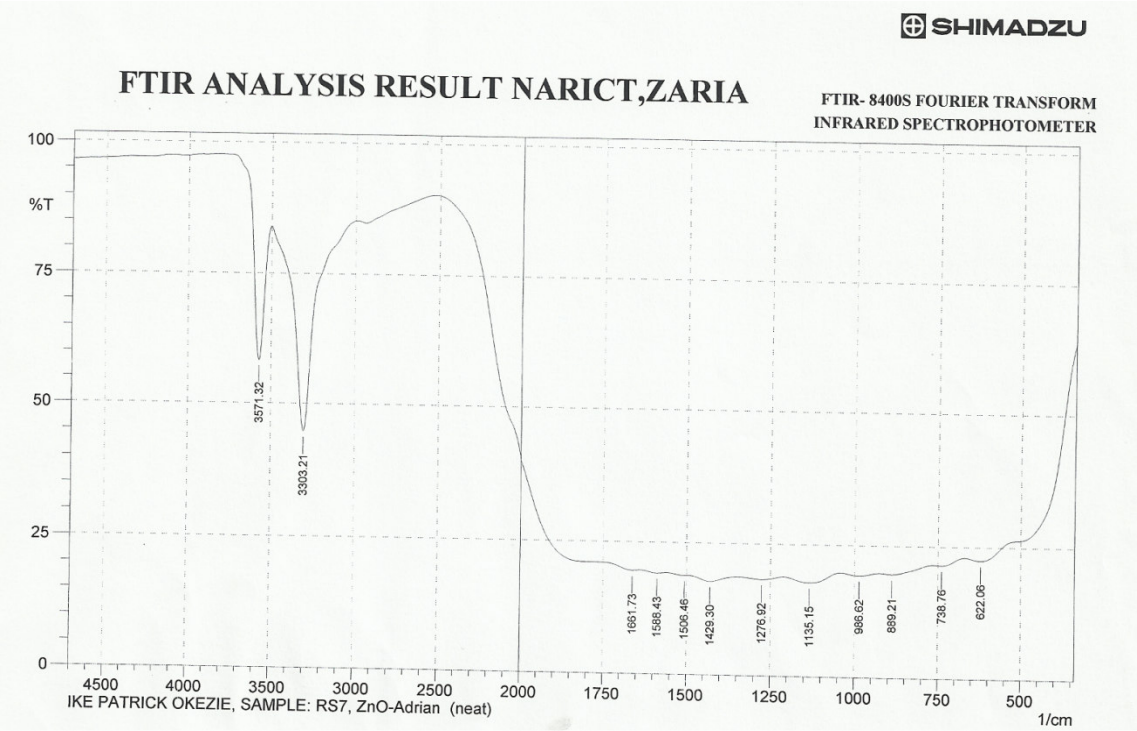

3.4 Structural Properties

In order to confirm the formation of CuO, and to study the crystal structures of the resultant films, XRD analyses were employed. The effect of bath pH and temperature on the preferred orientation of SILAR deposited Cu_xO on glass substrate was investigated. The presence of multiple peaks of the Cu_xO phase indicates the polycrystalline nature of films [21]. The XRD showed that two phases' cupric oxide (CuO) and cuprous oxide (Cu_2O) coexist depending on the pH of the solution bath.

Fig.10 (a-c) show typical XRD patterns of the thin film that were grown on glass substrates and deposited at room temperature for pH values 8, 9 and 11. For the CuO phase, the Miller-indexed (002) / (-111) and (1 1 1) / (2 0 0) reflections are the strongest, which indicate that they are preferential crystal planes of the nanostructures. While for the Cu_2O phase, the Miller-indexed (111) / (200) and (220) / (311) reflections are the strongest.

The crystallite sizes were calculated by the X-ray line broadening method using the Scherrer formula [31]: $D = k\lambda / \beta \cos\theta$, where λ is the wave length of radiation used (*CuK*α in this case), *k* is the Scherrer constant (0.9), β is the full width at half maximum (FWHM) intensity of the diffraction peak for which the particle size is to be calculated, θ is the diffraction angle of the concerned diffraction peak and D is the Crystallite dimension (or particle size).

At pH 8, two dominant peaks at 36.59º and 42.5º corresponding to the (111) and (200) planes of Cu_2O are seen with cubic crystal (JCPDS Card No. 05-0667). As the pH was increased to 9, all diffraction peaks can be clearly indexed to the monoclinic CuO phase with lattice constants of $a = 4.684$ Å, $b = 3.425$ Å, $c = 5.129$ Å, and $\beta = 99.47°$ (JCPDS Card No.: 05-0661). Finally, with the increase in the bath pH from 9 to 11, both phases were observed. Peaks associated with the monoclinic CuO showed a rise in intensity of the (002) and fall in the intensities of the (111), (2 00), (-2 02) and (-113), crystal planes respectively. The peaks at 42.29º and 73.52º can be assigned to (200) and (311) planes of Cu_2O.

The average crystallite sizes for films deposited at room temperature are: 1.52Å, 1.53Å and 1.64Å respectively.

Thus it is seen from the present investigation, that increasing the pH of copper complex solution leads to a mixed phase of CuO and Cu_2O.

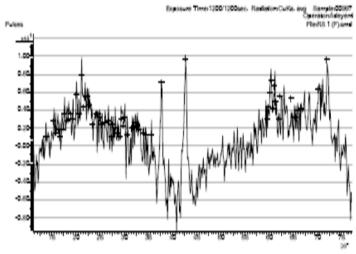

a

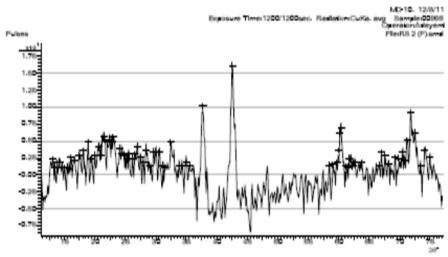

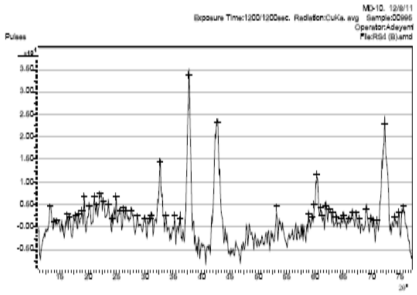

b c

Fig 10 (a-c) XRD patterns of the thin film that were grown on glass substrates and deposited at room temperature for pH values 8, 9 and 11.

Fig. 11 (a-c) shows the effect of heating the solution bath of the anionic precursor to 70°c on the structure of the film deposited at pH 8, 9 and 11. All diffraction peaks reveals the formation of single phase Cu_2O with cubic structure. The Miller-indexed (111) / (200) and (220) / (311) reflections are the strongest. The average crystallite size was calculated to be approximately 1.52Å, 1.54Å and 1.67Å respectively.

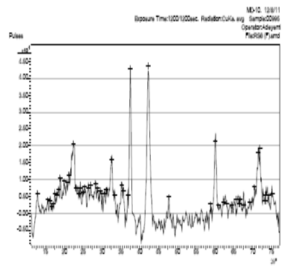

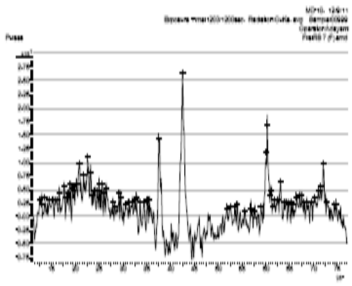

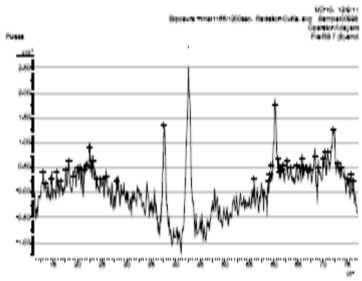

a b c

Fig. 11 (a-c) XRD patterns for film synthesized at a bath temperature of 70°c on glass substrate (a)= pH 8 (b) = pH 9 (c) = pH 11

Conclusion

In conclusion, we have synthesized polycrystalline Cu_xO films using a simple chemical method: successive ionic and layer adsorption reaction (SILAR) method. SEM micrograph revealed that the grains were evenly distributed over the substrate surface. XRD studies confirmed that the films were crystalline in nature with both Cu_2O and CuO crystallographic phases existing depending on the pH of the solution bath. The average crystallite size was found to be in the range, 1.52 - 1.67Å. The FTIR spectral showed that the Cu_2O phase was predominant. The bandgap energy value was found to be in the range, 1.6eV-2.0 eV

References

[1] G. Papadimitropoulos, N. Vourdas, V. Vamvakas Em and D. Davazoglou, *Thin Solid Films*, 515 (2006) 2428–2432.

[2] A. A. Ogwu, E. Bouquerel, O. Ademosu, S. Moh, E. Crossan, F. Placido, J. Phys. D Appl.Phys. 38, (2005) 266

[3] T.J. Richardson, J.L. Slack, M.D. Rubin, Proceedings of the 4th International meeting on Electrochromism,

Uppsala, (2000).
[4] A. Paretta, M.K. Jayaraj, A. Di Nocera, S. Loreti, L. Quercia, A. Agati, Physic Status Solidi A155\2 (1996) 399-404
[5] B. Balamurunga and Mehta B. R, *Thin. Sol. Films* 396 **(**2001)90
[6] K. H. Yoon, W. J. Choi and D.H. Kang, *Thin Solid Films*, 372 (2000) 250.
[7] D. P. Singh, Jai Singh, P. R. Mishra, R. S. Tiwari and O. N. Srivastava, *Bull. Matter. Sci*., 31(2008)319-325.
[8] M. Muhibbullah, M.O .Hakim, M.G.M. Choudhury, Thin Solid Films, 423 (2003)103
[9] J.R. Ortiz , T. Ogura, J. Medina-Valtierra, S.E. Acosta-Ortiz, P. Bosh , A. de las Reyes, V.H Lara., *Appl. Surf.Sci.*, 174, (2001) 177
[10] R.B., Vasiliev M.N. Rumyantseva, N.V. Yakovlev, A.M. Gaskov, Sens. Actuators, B, Chem. 50, (1998) 186,
[11] Nakamura Y., Zhuang H., Kishimoto A., Okada O.,Yanagida H., *J. Electrochem. Soc*. 145 (1998) 632
[12] P. Mitra, Journal of Physical Sciences, 14(2010), 235-240
[13] M. Schlesinger and M. Paunovic Wiley, New York, 2000
]14] A.Y. Oral, E. Mensur, M. H. Aslan and E. Basaran, *Mater. Chem. Phys*., 83 (2004) 140
[15] A. E. Rakshani , *Sol. St. Electron.* 29(1986) 7
[16] D. P. Singh, Jai Singh, P. R. Mishra, R. S. Tiwari and O. N. Srivastava, *Bull. Matter. Sci*.,**2008**, 31,319-325.
[17] Y. S. Gong, C. Lee and C. K. Yang, *J. Appl. Phys*., 77(1995) 5422**.**
[18] M. Parhizkar, S. Singh, P. K. Nayak, N. Kumar, K. P. Muthe, S. K. Gupta, R. S.Srinivasa, S. Talwar and S. Major, *Colloids Surf. A: Physicochem. Eng. Asp*. 257(2005) 277.
[19] M. Hari Prasad Reddy, P. Narayan Reddy and S. Uthanna, *Indian Journal of Pure and Applied Physics*, , 48(2010), 420.
[20] S. Szu and C. L. Cheng, *Mater. Res. Bull*., 43(2008) 2687.
[21] Y. Li, J. Liang, Z. Tao and J. Chen, *Mater. Res. Bull*, 43(2008) 2380.
[22] W. Shang, X. Shi, X. Zhang, C. Ma and C. Wang, *Appl. Phys*. A, , 87(2007) 129.
[23] T. Maruyama, *Jpn. J. Appl. Phys*, 37(1998) 4099,
[24] K. Santra, C.K. Sarkar, M.K. Mukherjee and B. Ghosh, *Thin Solid Films*, 213(1992) 226
[25] J.F. Pierson, A. Thobor-Keck, A.Billard, Applied surface science 210 (2003) 359-367.
[20] S. Ishizawa, T. Maruyama, K. Akimoto, Japanese Journal of Applied Physics 39/2 (2000) 786-788.
[21] R. Chandra, P. Taneja, P. Ayuub, Nanostructured Materials, 11/4 (1999) 505-512.
[22] S.C. Ray, Solar Energy Materials & Solar Cells 68\3-4 (2001) 307-312.
[23] T. Murayama, Solar Energy Materials & Solar Cells 56 (1998) 85-91.
[24] J. Yang, Z. Jin, T. Liu, C. Li and Y. Shi, *Solar Energy Materials and Solar Cells* **92** (2008) 621–627.
[25] G.F. Zou, H. Li, D.W. Zhang, K. Xiong, C. Dong and Y.T. Qian. *J. Phys. Chem.*, 110 (2006) 1632–1637.
[26] H. Derin, K. Kantarli, Applied Physics, Materials Science and Processing 75 (2002) 391-395.
[27] P. Luzeau, X.Z. Xu, M.Lagues, N. Hess, J.P. Contour, M. Nanot, F.Queyroux, M. Touzeau, D. Pagnon, Journal of Vacuum Science Technology 8/6 (1990) 3938-3940.
[28] C.H. Lu, L.M. Qi, Y.H. Yang, X.Y. Wang, D.Y. Zhang, J.L. Xie and J.M. Ma. *Adv. Mater.*, 17 (2005) 2562–2567
[29] T. Murayama, Solar Energy Materials & Solar Cells, 56 (1998) 85-91
[30] S.C. Ray, Solar Energy Materials & Solar Cells 68 (2001) pp 307-312.
[31] S. Ishizawa, T. Maruyama, K. Akimoto, Japanese Journal of Applied Physics 39 (2000) 786-788
[32] H. Klug and L. Alexander, Wiley, New York, 618 (1974)